

IONOSPHERIC CONVECTION AND THE SUBSTORM CYCLE

M. Lockwood¹

(Rutherford Appleton Laboratory, Chilton, Didcot, OX11 0QX, U.K.)

and S.W.H. Cowley

(Blackett Laboratory, Imperial College, London, SW7 2BZ, U.K.)

ABSTRACT

During substorms, magnetic energy is stored and released by the geomagnetic tail in cycles of growth and expansion phases, respectively. Hence substorms are inherently non-steady phenomena. On the other hand, all numerical models (and most conceptual ones) of ionospheric convection produced to date have considered only steady-state situations. In this paper, we investigate the relationship of substorms to convection. In particular, it is shown that a steady-state convection pattern represents an average over several substorm cycles and does not apply on times scales shorter than the substorm cycle period of 1-2 hours. The flows driven by the growth and expansion phases of substorms are an integral (indeed dominant) part of, as opposed to a transient addition to, the overall convection pattern.

1. INTRODUCTION

Over the past two decades, a number of models of the ionospheric convection pattern at high latitudes have been developed using data either from low-altitude polar-orbiting satellites (Refs. 1-6) or from ground-based radars (Refs. 7-10). Equivalent convection patterns have been derived from magnetometer data using models for the spatial distribution of ionospheric conductivities (e.g. Ref. 11). In addition to these numerical models of convection, several studies have combined simultaneous measurements from a large number of observatories (radar and magnetometer) with satellite data to produce "snapshots" of the flow pattern (Refs. 12-14), but this has only been possible for limited periods of intensive study. Another method has been developed which combines in-situ data from a pass of a satellite with global auroral images, based on the assumptions that the UV luminosity arises from regions of upward field-aligned current and the pattern of flow remains steady for the time taken for the satellite to traverse it (Ref. 15).

All the models of convection (Refs. 1-10) have been produced by combining data from different points of the invariant latitude - Magnetic Local Time (MLT) coordinate system for a given set of solar-terrestrial conditions (e.g. the polarity of the B_z and B_y components of the interplanetary magnetic field (IMF), the Kp planetary magnetic index, or the A_E auroral electrojet indices). All such models are inherently steady state

ones. In every case, the model will yield a certain value at a certain location for a given set of prevailing conditions and no account is taken of the history of those conditions over the period leading up to the time considered (see discussion given in Ref. 16).

On the other hand, substorms are a phenomenon which have long been considered in terms of departures from steady state (Refs. 17-26). For southward IMF, reconnection near the nose of the magnetosphere generates open flux which threads the magnetopause and is swept anti-sunward into the tail of the magnetosphere by the flow of the solar wind. This magnetic flux (and the corresponding magnetic energy) accumulates in the tail in the so-called growth phase of the substorm. In this way, the reconnection at the subsolar magnetopause results in the extraction of energy from the solar wind and its storage in the tail lobe. During this growth phase, the area of the ionospheric projection of the tail lobe, the ionospheric polar cap, expands. This is because the currents which flow in the ionosphere cause only minor changes in the ionospheric field strength, B_i (which is constant at about 5×10^5 T) - in other words, the ionosphere is essentially incompressible. Hence while reconnection at the dayside magnetopause increases the total amount of open flux, F , the ionospheric polar cap area, A_{pc} , increases at a rate given by

$$B_i (dA_{pc}/dt) = dF/dt = -\Delta V \quad (1)$$

where, by Faraday's law, ΔV is the e.m.f. around the boundary of the polar cap, in its own rest frame. Because convection models have up to now been inherently steady state, the time derivatives and hence the e.m.f. ΔV have been taken to be zero - i.e. polar cap expansion and contraction have not been taken into account.

The expansion of the polar cap during growth phases does not continue indefinitely: eventually, it is always halted and then reversed in the subsequent substorm expansion phase. Hence some process must then act to destroy the open flux at a rate which exceeds that at which it is generated at the dayside magnetopause. This is reconnection in the neutral sheet of the tail, which converts pairs of open field lines into closed field lines. This process liberates some of the energy stored in the tail lobe, which is deposited as particle heating in the plasma

¹ Also Visiting Honorary Lecturer, Blackett Laboratory, Imperial College, London, U.K.

sheet and in the ionosphere/thermosphere system. Equation (1) still applies, but ΔV has the opposite sense in this expansion phase (contracting polar cap) to that in the growth phase (expanding polar cap).

At this point, we note briefly that reconnection at the magnetopause can occur when the IMF is northward (possibly in one hemisphere at a time, in a manner controlled by the IMF B_x component and/or the time-of-year). The various magnetic topologies possible during northward IMF are discussed by Cowley (Refs. 27, 28) and their implications for convection have been recently evaluated by Crooker (Ref. 29). These topologies involve reconnection at the magnetopause of the (northward) magnetosheath field with either open or closed field lines on the outer edge of the tail lobe. However, following a northward turning of the IMF these outer lobe field lines will be open (generated by the prior period(s) of southward IMF) and hence, considering the variability of the IMF B_x polarity (Refs. 30-32), we believe that the reconnection will usually involve already-open flux of the tail lobe. Hence this process reconfigures existing open field lines, but does not generate any new open flux. In doing so, it drives "stirring" flows in the highest latitude ionosphere and some direct energy deposition; however, it does not contribute to ΔV nor to the storage of energy in the tail lobe. For this reason, substorm growth phases occur exclusively during periods of southward IMF: however, note that expansion phases will continue to destroy open flux and deposit stored energy after the IMF has turned northward, but that these will almost certainly decay in magnitude while the IMF remains northward.

Hence there is a fundamental difference between the concept of convection, as tacitly advocated by existing models of the patterns of ionospheric flows, and the accepted concepts of energy storage and release during the substorm cycle. The purpose of this paper is to show how the two concepts can be reconciled with simple allowance for non-steady conditions and to discuss the implications.

2. GENERAL CONCEPTS

As early as 1972, Russell (Ref. 25) sketched separately the ionospheric flows associated with the non-steady conditions of growth and expansion phases of substorms. However, this concept was not used again as an aid to understanding ionospheric convection for a further 15 years. Then Siscoe and Huang (Ref. 33) quantified the flows for the first-order simplification of a circular polar cap. These authors also introduced the very important concept of "adiarctic" (meaning "not flowing across") segments of the polar cap boundary between open and closed field lines. As discussed in the introduction, this boundary must, in general, move as the polar cap expands and contracts during the substorm cycle.

2.1 Adiarctic polar cap boundaries.

The boundary between open and closed field lines can have one of two forms. Flux tubes can cross this boundary at segments called the "merging gaps". Because reconnection is

the only way of converting open field lines to closed (and the reverse), the merging gaps must, by definition, be the ionospheric projections of the X-lines in the magnetosphere at which reconnection occurs. However, reconnection is not expected at all MLT, nor at all times. When and where reconnection is not taking place, no flux tubes can convect across the boundary and the field lines project to an ionospheric polar cap boundary that is adiarctic.

Figure 1 demonstrates an important consequence of adiarctic boundaries which move. The dashed lines show the location of a segment of the open/closed field line boundary at three times (t_1 , t_2 and t_3). This segment is considered to be adiarctic at all times (i.e. no flux tubes convect across the boundary because no reconnection is taking place at the range of MLT shown). Hence at all points where the boundary moves, the plasma immediately adjacent to the boundary has a component of its velocity normal to the boundary which equals the speed of the boundary motion. Hence the flow streamlines cross the boundary, even though no reconnection is taking place locally and no plasma or flux tubes convect across the boundary. In figure 1, the flow streamlines show an arbitrary flow cell, consistent with the boundary motion. It is important to note that this flow cell is not confined to either the open or the closed field line region, rather the flow streamlines move from one to the other and back, without any reconnection taking place.

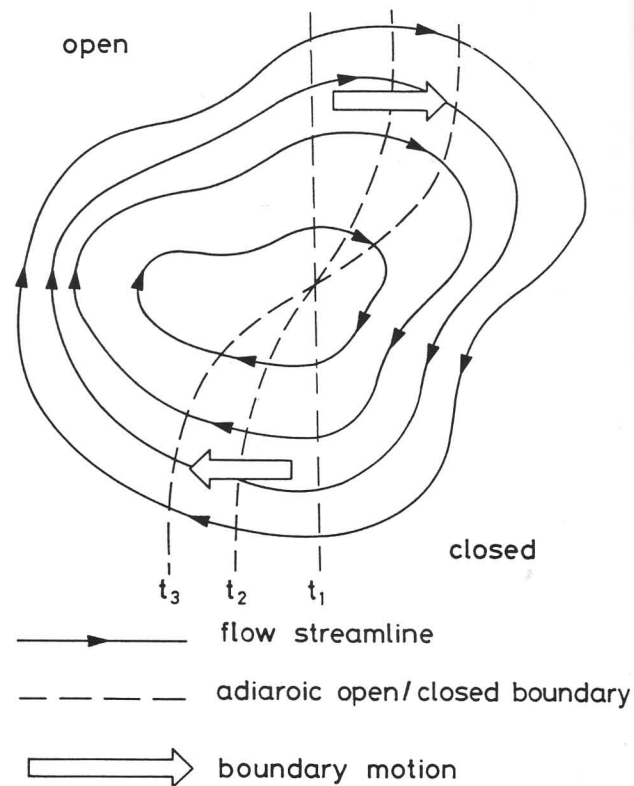


Fig. 1. Illustrative ionospheric flow cell showing streamlines crossing a moving adiarctic open/closed field line boundary.

In many conceptual models (e.g. that by Reiff and Burch, Ref. 34), the flow streamlines only cross the open/closed boundary at merging gaps. Figure 1 demonstrates that this is not the case if the boundary is in motion. Therefore, models for which streamlines only cross the open/closed boundary at merging gaps are also inherently steady-state ones - no allowance has been made for boundary motions (as, for example, expected as the polar cap expands and contracts during the substorm cycle).

Note that flux tubes cannot circulate completely around a flow cell of the type demonstrated in figure 1: hence the cell cannot keep the same form over an extended period. This contrasts with the steady state case, where open flux tubes could circulate indefinitely around a ("lobe") flow cell confined within the polar cap and closed field lines could circulate indefinitely around a ("viscous") cell a latitudes outside the polar cap. Circulation from closed to open field lines and back can continue indefinitely in steady-state "merging cells".

2.2 Flow, reconnection and transpolar voltages

Figure 2(a) shows schematically the magnetosphere, and Figure 2(b) the ionospheric polar cap for southward IMF. Open field

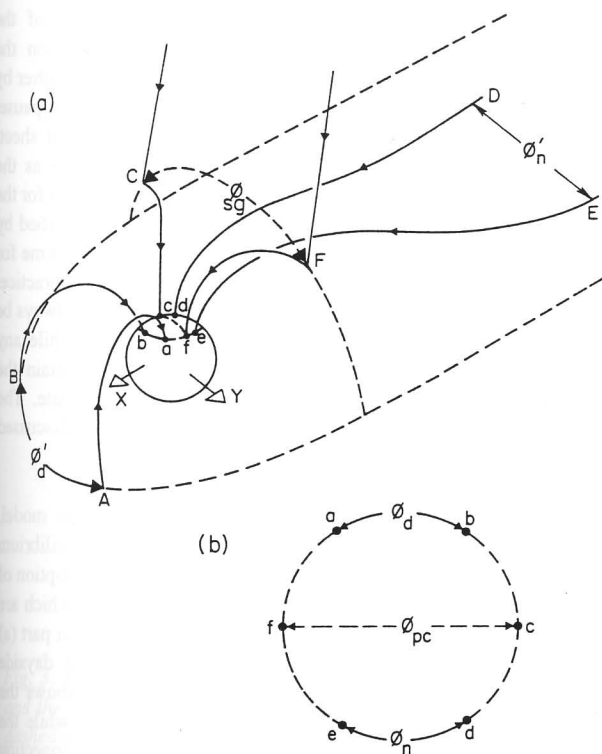


Fig. 2. (a) The magnetosphere, showing the dayside magnetopause X-line, AB, the nightside neutral sheet X-line, DE, and the "Stern Gap", CF. Solid lines are magnetic field lines, dashed lines lie in the magnetopause. Field lines map to the ionospheric polar cap, which is viewed from above the pole in (b). The dayside merging gap (the ionospheric projection of AB) is ab, the nightside merging gap (projection of DE) is de and the dawn-dusk diameter of the polar cap is cf (from Ref. 44).

lines are generated at the X-line on the dayside magnetopause, AB. This is shown here as lying in the equatorial plane, consistent with observations of the resulting accelerated flows (Ref. 35). Let us call the rate at which open flux is produced by this X-line in its own rest frame. By the definition of the merging gap, the flux transfer rate across the corresponding merging gap ab (i.e. the voltage along ab in its own rest frame) must also equal ϕ'_d . This analysis neglects any field-aligned voltages; however, auroral observations show that any such voltage would typically be about 1 kV, which is very small relative to the typical reconnection voltages. Likewise reconnection in the tail neutral sheet destroys open flux at a rate ϕ'_n , the rest-frame voltage across the nightside X-line DE and its corresponding merging gap de. Because we do not expect the magnetopause and tail X-lines to be contiguous, there are adiaric segments of the ionospheric polar cap boundary, bd and ae, where no flux is transferred across the boundary: consequently, there is no voltage along these segments in their own rest frame. Hence integrating around the polar cap boundary, we find that the total e.m.f is (by equation 1):

$$-\Delta V = \phi'_d - \phi'_n = dF/dt = B_i (dA_{pc}/dt) \tag{2}$$

This equation is simply Faraday's induction law applied to the ionospheric polar cap boundary. Alternatively, it can be thought of as a continuity equation - that of the open flux.

Let us first consider a steady state convection pattern, i.e. a convection pattern which takes no account of the phase of the substorm cycle. We know that on long time scales the polar caps neither expand to cover the entire Earth, nor do they disappear completely. Hence the long-term average of (dA_{pc}/dt) is zero and hence, by equation (2), we know that ϕ'_d equals ϕ'_n , when averaged over this timescale. For steady state conditions the rate at which open flux is transferred from the dayside X-line to the nightside X-line must equal the rate at which it is created and destroyed. In other words, the voltage across the "Stern gap" (CF), ϕ_{sg} , is also equal to $\phi'_d (= \phi'_n)$. In steady state the polar cap boundaries do not move and hence the voltages along the merging gaps ab and de, in the Earth's frame of reference (ϕ_d and ϕ_n , respectively) are the same as those in their rest frames (ϕ'_d and ϕ'_n). Likewise, applying Faraday's law to the circuit cCff shows that the dawn-dusk transpolar voltage (between c and f), ϕ_{pc} , equals ϕ_{sg} for steady-state conditions. Hence for steady-state models, which average over the substorm cycle, the voltages ϕ_d , ϕ_n , ϕ'_d , ϕ'_n , ϕ_{pc} and ϕ_{sg} are all equal.

Equation (2) shows us that for steady-state to apply, the reconnection voltages ϕ'_d and ϕ'_n must be equal. However, there is no reason to expect this to be the case, in general. The rate of dayside reconnection is known to depend on the magnetic shear across the dayside magnetopause, and several other factors. Similarly the rate of nightside reconnection will depend on a number of factors, including the magnetic shear across the tail neutral sheet. Cowley and Lockwood (1992) have pointed out that information about the voltage ϕ'_d cannot reach the site of the tail reconnection (DE) for at least 30 min.

Studies of the IMF show that the B_z component (and hence the shear across the magnetopause) remains constant for such a period or longer only about 50% of the time (Refs. 30-32). Hence ϕ_d' would generally alter in magnitude before ϕ_n' could attain equilibrium with it - even if some mechanism to equalise these two voltages were active. Hence we would generally expect ϕ_d' and ϕ_n' to differ at any one instant of time and hence the polar cap to be either expanding or contracting in size. There may be exceptions to this, however. For example, the magnetosphere sometimes reaches a long-lived, high-flow state with ϕ_d' and ϕ_n' large and roughly equal. This is called a "convection bay" and may relate to a period of unusually stable IMF. However, even for periods of northward IMF, the magnetic shear across the tail neutral sheet persists and hence tail reconnection continues, probably as a series of weakening bursts, even though ϕ_d' is small or zero. Hence steady state will not generally be a good approximation, even when the IMF is northward.

Hence we generally expect large departures from steady state, particularly during substorms. From equation (2), the polar cap area must change and hence its boundaries move in the Earth's frame of reference. As a result, the voltage across the adiaroic segments ae and db are not zero in the Earth's frame, and the flow voltage across the dayside merging gap ϕ_d is not equal to ϕ_d' nor is ϕ_n equal to ϕ_n' . If we consider uniform motion of a segment in the polar cap boundary, at speed v_b , the voltage in the Earth's frame equals that in the rest frame plus $(v_b B_i l)$, where l is the length of the segment. Hence, for example, the dayside reconnection voltage ϕ_d' will not cause any flow in the ionosphere (i.e. ϕ_d is zero) if the merging gap ab moves equatorward at a speed $v_{ab} = \phi_d' / (B_i l_{ab})$. In general, we know that the application of a dayside voltage causes the dayside cusp and the open/closed boundary to migrate equatorward (Ref. 36, 48) and hence we expect $\phi_d < \phi_d'$, while $\phi_n' > \phi_n$. Siscoe and Huang made the simplifying assumption that the polar cap is circular at all times (with a variable radius r). For this simple case, we find that (Ref. 16) the merging gap velocities (positive equatorward) are given by

$$v_{ab} = v_{de} = v_b = (\phi_d' - \phi_n') / (2\pi r B_i) \quad (3)$$

and the voltages in the Earth's frame by:

$$\phi_d = \phi_d' - (l_{ab} / 2\pi r) (\phi_d' - \phi_n') \quad (4)$$

$$\phi_n = \phi_n' - (l_{de} / 2\pi r) (\phi_n' - \phi_d') \quad (5)$$

$$\phi_{pc} = \phi_v + (\phi_d + \phi_n) / 2 \quad (6)$$

where ϕ_v is due to any viscous-like interaction. Note that for non-steady conditions, the polar cap voltage ϕ_{pc} does not equal ϕ_{eg} , in anything other than an average sense.

2.3 The expanding-contracting polar cap convection model

The example of non-steady convection presented by Siscoe and Huang (Ref. 33) was for wholly unbalanced dayside reconnection (i.e. $\phi_d' > 0$ and $\phi_n' = 0$). Moses et al. (Ref. 37)

modelled the flow during substorm expansion phases by considering wholly unbalanced nightside reconnection (i.e. $\phi_n' > 0$ and $\phi_d' = 0$): the results compared very favourably with data from selected satellite passes during expansion phases. Lockwood and Freeman (Ref. 38) generalised these two cases by sketching the flows for both expanding ($\phi_d' > \phi_n' > 0$) and contracting ($\phi_n' > \phi_d' > 0$) polar caps. All these are examples of predictions of the "Expanding-Contracting Polar Cap" (ECPC) convection model - also referred to as the "Two-Source" convection model (Ref. 16, 39).

A major success of the ECPC model has been to explain the response times of dayside ionospheric flows to changes in the IMF B_z component, as observed by the EISCAT radar, in conjunction with the AMPTE-UKS and -IRM satellites when immediately upstream of the Earth's bow shock (See Ref. 39 and references therein).

The limitation of the Siscoe and Huang model is the assumption that the polar cap remains circular, which prescribes the motion of the merging gap and the flow pattern. Cowley and Lockwood (Ref. 40) have recently provided a new concept which opens possibilities of generalising for any distortions of the polar cap from circular and allows the effects of a range of merging gap motions to be modelled. This concept is of zero-flow equilibrium configurations of the magnetosphere-ionosphere system, which depend upon the amount of open flux. If the total open flux is altered, either by the generation of new open flux at the dayside magnetopause, or the destruction of old open flux in the tail neutral sheet, flow is excited in the ionosphere and magnetosphere as the system tends towards the new equilibrium configuration for the new amount of open flux. If the system is only perturbed by a short single burst of reconnection, the characteristic time for the resulting flows to decay is of order 10-15 min. In practice, even if the dayside reconnection vanishes, there will always be some reconnection continuing in the tail (at least while any open flux remains). Hence the system will never attain the equilibrium, and flows will never completely stagnate. The evidence for, and implications of, this concept are discussed further by Cowley et al. (Ref. 41, this issue).

Figure 3 considers the convection predicted by this model, with the simplifying assumption that the equilibrium configurations of the polar cap is circular. (In fact, adoption of this simplifying assumption yields flow predictions which are the same as given by the Siscoe and Huang model). In part (a) we consider the flows driven by wholly unbalanced dayside reconnection ($\phi_d' > 0$ and $\phi_n' = 0$). The solid line shows the adiaroic polar cap boundary at an instant of time, while the dashed segment shows the merging gap at which reconnection is proceeding. The dot/dash line shows the equilibrium polar cap boundary: were the reconnection to cease (so the amount of open flux was no longer altered), over the subsequent 10-15 min. the polar cap boundary would move to this location and the flows would disappear. The ongoing reconnection means that at all times the merging gap lies equatorward of the equilibrium boundary, whilst at all other local times the boundary lies poleward of its equilibrium location. Hence poleward flow is excited at the merging gap and equatorward flow elsewhere, yielding the flow streamlines shown. Note that

the flow streamlines cross the expanding adiaroic segment of the polar cap boundary.

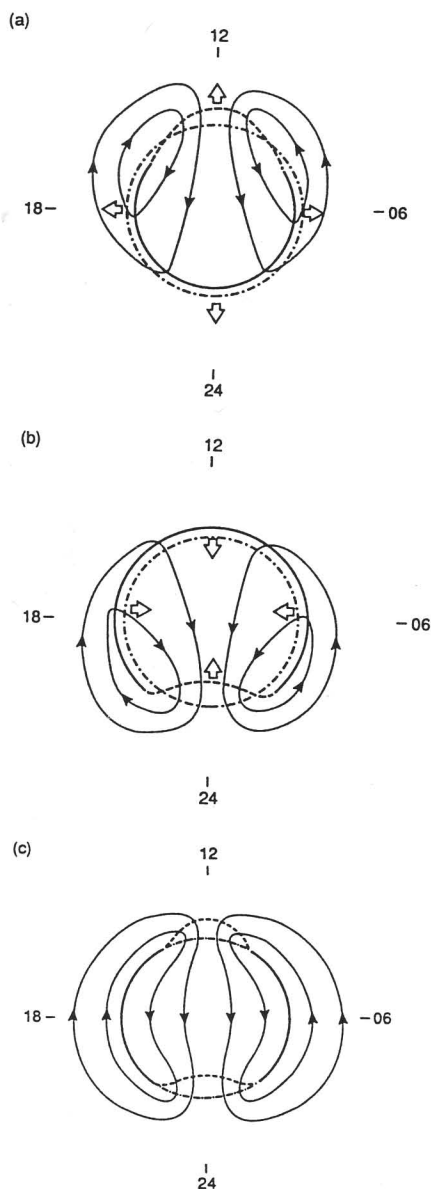


Fig. 3. The ionospheric flows predicted by the ECPC model and the flow excitation model of Cowley and Lockwood. The dashed segments of the polar cap boundary are merging gaps, the solid segments are adiaroic. The dot-dash line is the zero-flow equilibrium boundary for the open flux present. For simplicity the polar cap is considered to remain circular and open arrows denote the direction of boundary motion. (a) $\phi_d > 0$, $\phi_n = 0$; (b) $\phi_n > 0$, $\phi_d = 0$; (c) $\phi_n = \phi_d > 0$ (from Ref. 40).

Part (b) of figure 3 shows the flows driven by wholly unbalanced nightside reconnection ($\phi_n' > 0$ and $\phi_d' = 0$). The application of the same principles yields a similar form of flow pattern. Note that a two-celled flow pattern is generated in

both cases - although reconnection is ongoing at only one site in both cases.

The part (c) of figure 3 shows the special limit where ϕ_n' and ϕ_d' are equal. By equation (2) this is the steady-state case and hence the polar cap boundaries no longer move. As described above, this means that the flow streamlines no longer cross the adiaroic segments of the polar cap boundary.

The flow patterns in figure 3 could be easily generalised were the equilibrium boundary contour not to be circular, such that the boundary speed varied with MLT. Streamlines which cross the adiaroic boundary would be bunched together where the boundary moved faster, and further apart where it moved slower. In addition, we can allow for both dayside and nightside reconnection occurring but at different rates. Some general principles are that for an expanding polar cap ($\phi_d' > \phi_n'$), the convection cells are centred on the ends of the dayside merging gap, as in 3(a); whereas for a contracting polar cap ($\phi_n' > \phi_d'$) they are centred on the ends of the nightside merging gap, as in 3(b). The special case of steady state ($\phi_d' = \phi_n'$) is achieved only for brief periods as the dayside and nightside reconnection rates vary, and also applies to long term averages, as described above. Then the flow cells are centred near dawn and dusk. The shift of the flow cell centres to the nightside for dominant nightside reconnection has been verified by the evolution of the flow pattern, as derived from global radar and magnetometer data using the AMIE technique (Ref. 14), following a northward turning of the IMF (see discussion given in Ref. 42).

Lastly, we note that the discussion here takes no account of dawn-dusk asymmetries in the flow pattern, associated with the B_y component of the IMF. Such asymmetries are readily introduced on the dayside by consideration of the tension forces on newly-reconnected field lines. In addition, the patterns of flow will be altered by the spatial distribution of the ionospheric conductivity (see Ref. 41).

3. CONVECTION DURING THE SUBSTORM CYCLE

3.1 Isolated substorms

Figure 4 shows the possible behaviour of various parameters during and following a period of southward IMF lasting 1-2 hours, as shown in the temporal variation of B_z in the top panel. Were the dayside reconnection rate ϕ_d' to depend purely on the magnetic shear across the dayside magnetopause, it would have the variation shown in the second panel. Observations show that the nightside reconnection rate does not respond to the southward IMF for a period of order 1 hour. Here, we indicate that ϕ_n' then grows to a greater voltage than ϕ_d' , so that the polar cap begins to shrink, shortly prior to the cessation of dayside reconnection, due to the return of the IMF to a northward orientation. The fourth panel gives the evolution of the polar cap flux, F , as given by equation (2). We can relate various times and periods in this sequence to an isolated substorm cycle, as shown in the figure: a is the onset of the growth phase (interval b); c is the onset of the expansion phase (interval d); and e is the recovery phase.

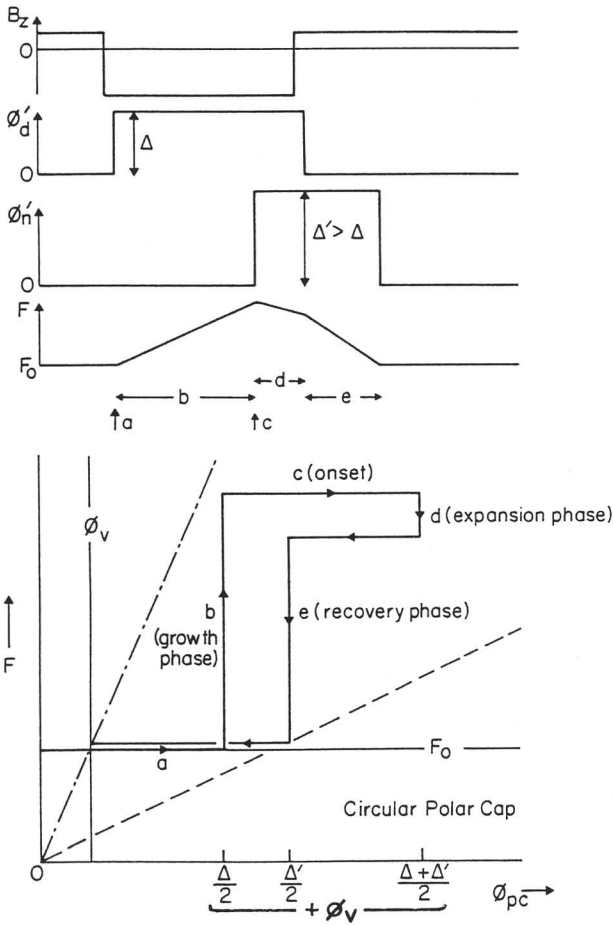


Fig. 4. Variation with UT of the IMF B_z , the reconnection voltages ϕ_d' and ϕ_n' and the open flux, F , for a simple model of an isolated substorm. The bottom panel shows the predicted variation of F with transpolar voltage, ϕ_{pc} (from Ref. 44).

The plot at the base of figure 4 considers how the polar cap flux will vary as a function of the dawn-dusk transpolar voltage ϕ_{pc} . For simplicity, the polar cap has been assumed to be circular, and the dayside merging gap to have the same length as the nightside merging gap ($l_{ab} = l_{de}$). Equations (4)-(6) then show that ϕ_{pc} is the arithmetic mean of ϕ_d' and ϕ_n' . In figure 4 we have added a small voltage ϕ_v which is due to viscous-like interaction. It can be seen that these two parameters vary in a characteristic way during the isolated substorm, which will be discussed further later.

In the growth phase, the polar cap expands as reconnection at the dayside magnetopause proceeds, but that in the tail is at a low level. Hence the flow pattern during the growth phase should have the general form of figure 3(a), with additional features caused by factors such as non-circular equilibrium boundary, the effects of IMF B_y and non-uniform ionospheric conductivity, and non-zero nightside reconnection rate. Importantly, the convection cells will be centred on the dayside (at the ends of the dayside merging gap). In the expansion phase, reconnection proceeds faster in the tail than

on the dayside and the polar cap contracts. Hence the flow pattern will still show a two-celled form but with those cells centred on the nightside (at the ends of the nightside merging gap), as in figure 3(b).

Figure 5 shows two flow patterns which were derived during a substorm cycle on 22 March 1979. This substorm was part of the CDAW-6 study (Refs. 20, 43, 45) and has recently been re-analysed in the light of the ECPC convection model by Lockwood (Ref. 44). The patterns were derived from 1-minute magnetometer data using the KRM inversion technique, as described for this day by Kamide and Baumjohann (Ref. 45).

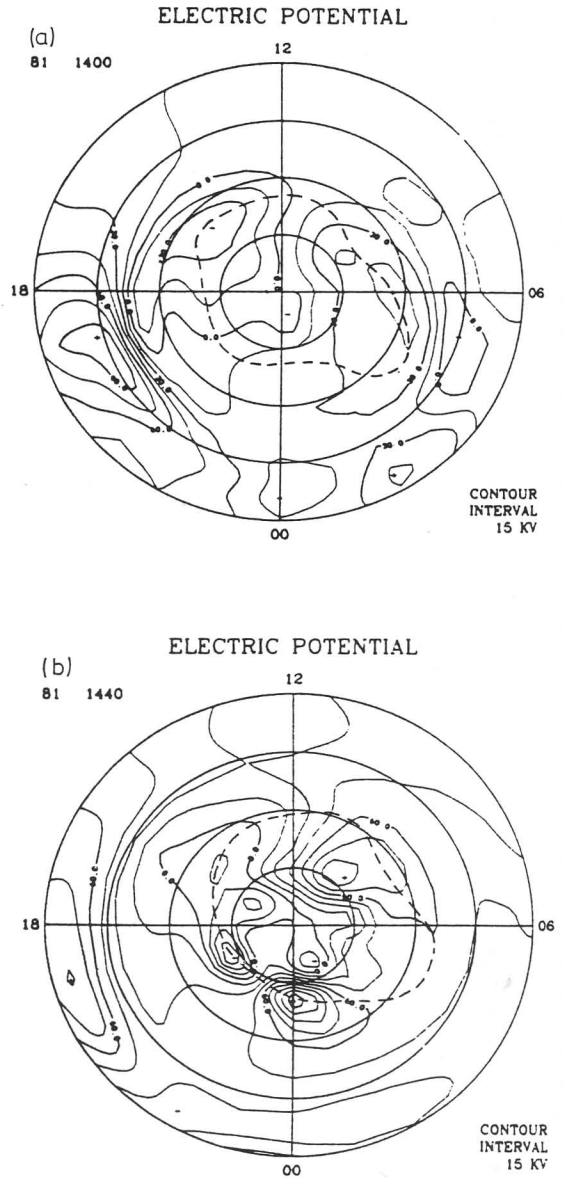


Fig. 5. Flow streamlines (equipotentials) computed by the KRM magnetogram inversion technique for 22 March, 1979 (a CDAW-6 interval). (a) For 14:00 UT, in the growth phase of a substorm; (b) for 14:40 UT, in the subsequent expansion phase (from Refs. 44, 45).

In figure 5(a) the expected bunching of the flows cells on the dayside is clearly evident during the growth phase. In 5(b) the dayside flow has not radically altered; however, the peak voltage now appears across a small segment of the nightside convection boundary. We would associate this segment with the merging gap. The patterns in figure 5 do not appear exactly the same as those predicted in figure 3. However, this is not surprising considering the number of complicating factors omitted from the model plots, as discussed above. In addition, there are uncertainties in the flows derived from the magnetometer data, principally due to the assumed spatial distribution of conductivity. However, the flow patterns do show that the concepts of convection in the growth and expansion phases, as put forward by the ECPC model, are substantially correct.

It is interesting to compare this substorm with the idealised behaviour discussed in figure 3. In order to do this, the transpolar voltage, ϕ_{pc} has been scaled from the potential contours (such as those given in figure 5), along the dawn-dusk meridian. In addition, the polar cap flux, F , was estimated by assuming a circular polar cap, with diameter equal to the separation of the 6 MLT and 18 MLT convection reversal boundaries. The variation of F with ϕ_{pc} during both the substorms on 22 March 1979 is shown in figure 6. The behaviour during the first of the two substorms (i.e. that addressed in figure 5) is very similar to that predicted by the simple considerations of figure 4. The second (larger) of the two substorms does not fit this simple sequence quite so well,

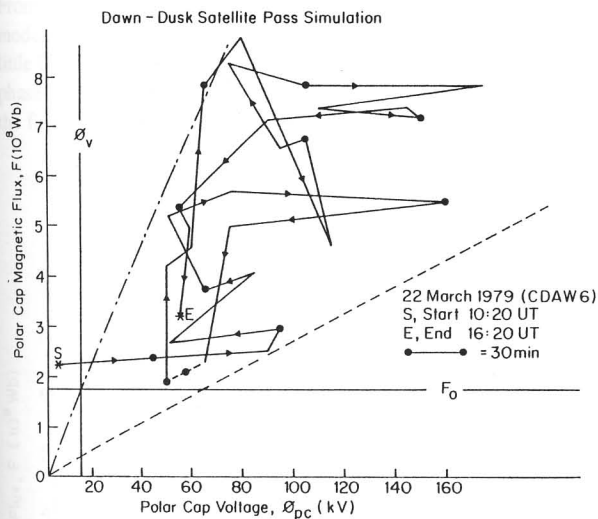


Fig. 6. Variation of open flux, F , with transpolar voltage, ϕ_{pc} , for the period 10:20-16:20 UT on 22 March 1979, showing the two isolated substorms of the CDAW6 periods (from Ref. 44).

showing an apparent drop in F and recovery close to onset of the expansion phase. However, close inspection reveals that this is merely due to a departure of the convection polar cap from circular, such that the assumptions employed yield a value for F which is too low.

Hence the isolated substorms on 22 March 1979 (CDAW6)

provide strong evidence that convection varies during the substorm cycle in the manner predicted by the ECPC model.

From analysis of convection patterns, such as those shown in figure 5, Lockwood (Ref. 44) has located the merging gaps for each flow snapshot. By comparing successive flow snapshots the motion of the merging gaps was determined. Hence on the dayside, the merging gap voltage in both the Earth's frame (ϕ_d) and in the merging gap rest frame (ϕ'_d) were obtained. Likewise, the nightside voltages ϕ_n and ϕ'_n were obtained. Because of the merging gap motions, and the consequent induction electric fields, the voltages observed in the ionosphere (ϕ_d and ϕ_n - which influence the terrestrial polar cap observations such as ϕ_{pc} and the A_E indices) are significantly different to the reconnection voltages (ϕ'_d and ϕ'_n).

Figure 7 shows the deduced reconnection voltages ϕ'_d (top) and ϕ'_n (bottom) as dashed lines and compares them with the IMF B_z component during the first substorm on 22 March 1979. In the top panel the B_z variation has been shifted by 12.5 min. to allow for the propagation time from the solar wind monitor (IMP-8) to the dayside ionosphere. The behaviour of dayside

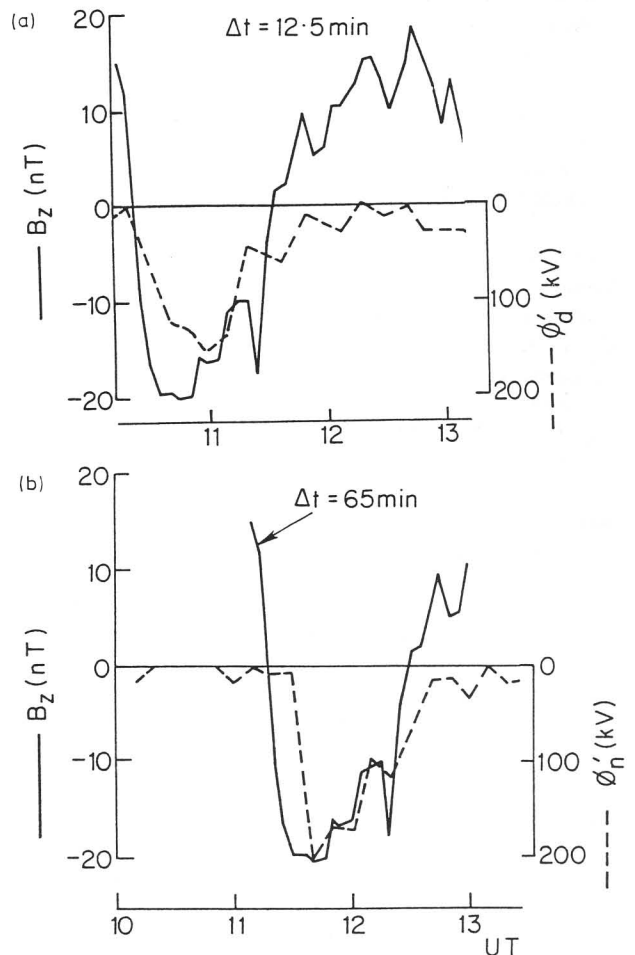


Fig. 7. Estimated reconnection voltages on (a) the dayside, ϕ'_d , and (b) the nightside, ϕ'_n , as a function of UT (dashed lines). The solid lines show the IMF B_z component (in GSM) observed by IMP-8, lagged by 12.5 in (a) and 65 min. in (b) (Ref. 44).

voltage is consistent with that inferred from the EISCAT-AMPTE observations (Ref. 39). In the bottom panel an arbitrary lag of 65 min has been introduced. It can be seen that both ϕ'_d and ϕ'_n show a similar variation to B_z but that ϕ'_n lags after ϕ'_d by about 50 min. This "directly-driven" behaviour was not at all clear in the variations of ϕ_n , ϕ_{pc} nor A_E , which are all measured in the Earth's frame of reference. It appears that the nightside reconnection voltage was, in this case at least, directly driven by the IMF B_z component of the IMF, but the ionospheric response was complicated by the induction effects (i.e. magnetic field changes within the magnetosphere). The variation of the voltage appearing in the ionosphere was different from the reconnection voltage because the merging gap motions. On the nightside this was because, in broad terms, the merging gap initially moved equatorward during the expansion phase so that $\phi_n > \phi'_n \approx 0$. About 30 min. after onset the reconnection burst began and the merging gap retreated poleward again, giving $\phi_n < \phi'_n$. Hence the reconnection pulse in the tail was considerably smoothed and complicated by these merging gap motions. Note that open flux was not destroyed until about 30 min. after onset. Equatorward erosion and subsequent poleward retreat of the dayside merging gap had a corresponding effect on the dayside flow response. Similar, although slightly less clear, behaviour was obtained for the following substorm on this day; however, the best fit to ϕ'_n was obtained by lagging B_z by a shorter delay of 45 min. The reasons for this difference are not yet clear. The finding of two separate response times of order 10 min. and 1 hour is consistent with previous statistical studies of substorms, for example by Baker et al. and Bargatze et al. (Refs. 18 and 19).

This analysis is open to some possible error, arising from the assumed conductivity distribution used to derive the flow patterns and from the identification of the polar cap boundary. However, it is difficult to see how such errors could have produced the results obtained. Evidence supporting the conclusions comes from the derived variation of the open flux, F , with time [computed from the integral of $(\phi'_d - \phi'_n)$ with respect to time] which is like that for the simple model as shown in figure 4. This variation is similar in form to that deduced for the same substorm by Holzer et al. (Ref. 20) from the auroral/polar cap boundaries, as determined from particle observations by two DMSP satellites. However, it is highly significant that both F and dF/dt are much smaller than deduced by Holzer et al. - implying that the open/closed boundary lies poleward of the auroral boundaries they defined.

3.2. Substorms during Northward IMF

As discussed earlier, the most likely magnetopause reconnection during periods of northward IMF involves open field lines in the tail lobe. This stirs open field lines in the polar cap and introduces a circulation. Figure 8(a) shows the ionospheric convection pattern for the case where this is the only reconnection taking place. Outside the lobe circulation in the polar cap are drawn two viscously-driven cells on closed field lines (see e.g. Ref. 34). Because no open field lines are created or destroyed, the polar cap neither expands or contracts, i.e. this is a steady-state case. Hence the open/closed boundary is everywhere adiarocic and stationary. Hence in this case the lobe circulation is entirely on open field lines within

the polar cap and any viscous cells are entirely on closed field lines.

However, it is unlikely that the reconnection X-line in the tail is completely dormant as long as any open flux exists. The open flux accumulated while the IMF was southward would be expected to yield a series of substorms, at progressively higher latitudes and of ever smaller magnitude, as the amount of open flux decays and the polar cap shrinks. During one of these northward IMF substorms the polar cap will shrink and convection would take on the form shown in figure 8(b). In this case, the lobe stirring and viscous interaction are both still active, but flow cells are not confined to either the open or the closed field line region because the boundary is shrinking poleward.

Figure 8(c) shows the same situation, but with no viscous-like interaction mechanism active. The only difference with 8(b) is that the dayside convection boundary reversal now lies on the open/closed boundary, instead of slightly equatorward of it.

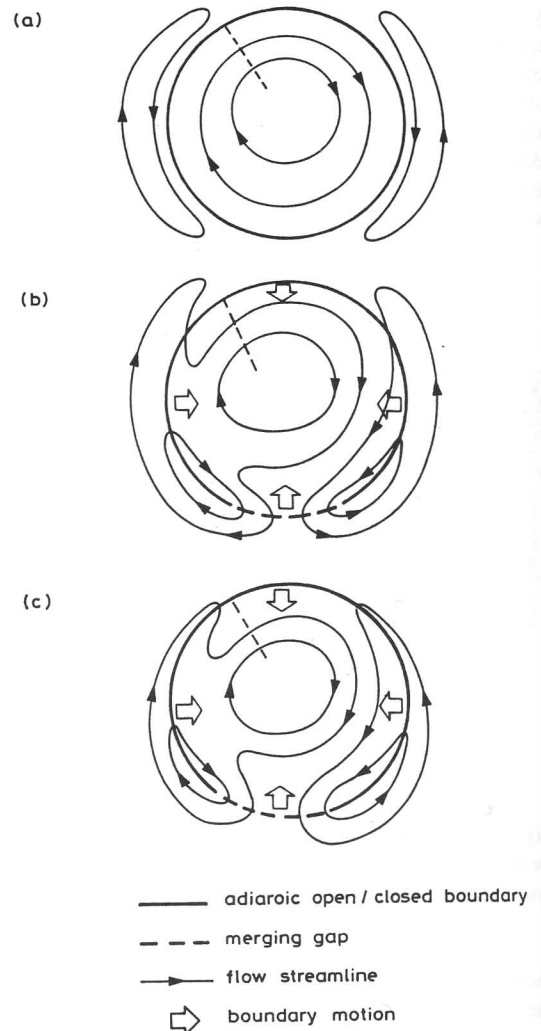


Fig. 8. Flow patterns for northward IMF: (a) a steady-state ($\phi'_d = \phi'_n = 0$) and (b and c) during a northward-IMF substorm ($\phi'_d = 0$, $\phi'_n > 0$). In (b) viscous interaction is active on closed field lines, in (c) it is not.

Because in most cases it would be impossible to tell the difference between 8(b) and 8(c), it is entirely possible that flows previously attributed to some viscous-like interaction mechanism were driven by weak reconnection continuing in the tail of the magnetosphere. This consideration complements the findings of Wygant et al. (Ref. 46), who showed that the peak transpolar voltage decayed to very low values about 9 hours following a northward turning of the IMF. Prior to this the voltage could be large or small. Figure 8 would suggest that the larger values were taken during northward-IMF substorm expansions, while the lower values were not. After the 9 hours, the repeated (and weakening) substorms have greatly depleted the polar cap. For many satellite passes, the flows would be indistinguishable from the steady-state case 8(a).

It is interesting to note that the flow pattern derived by Marklund et al. (Ref. 15) for a northward-IMF polar cap showing a transpolar arc, has many similarities to those sketched here in Figures 8(b) and 8(c). The derived flows are based on the field-aligned currents inferred from a pass of the VIKING satellite and a global UV auroral image, and match those observed by VIKING, HILAT and DMSP-F7 reasonably well; hence it can be considered as an average over the pass durations of about 10 min., which may have been part of the expansion phase of a northward IMF substorm.

4. WHAT IS CONVECTION?

From the above, it is evident that steady-state convection models can only be applied in an average sense and have very little bearing on the "instantaneous" flows observed at any one phase of the substorm cycle. The ECPC model predicts that the flow pattern will oscillate during the substorm cycle with

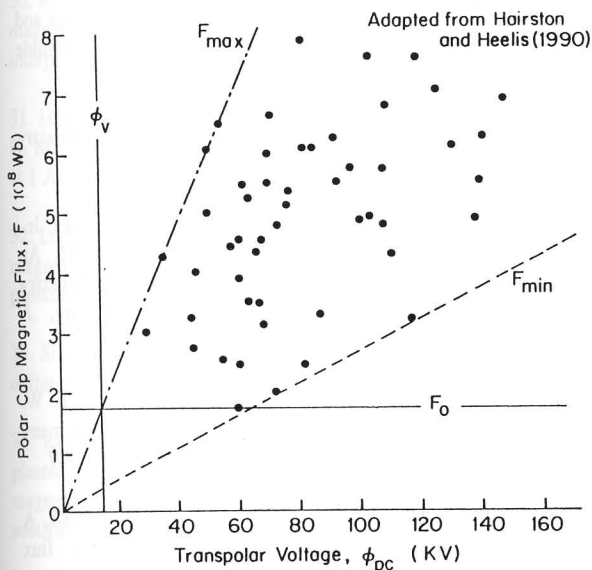


Fig. 9. Polar cap flux, F , as a function of transpolar voltage, ϕ_{pc} from convection observations by the DE-2 satellite (from Refs. 6 and 44)

dayside flows dominating during the growth phase (the "directly-driven" flows which accompany the storage of energy in the tail and are required for the associated polar cap expansion) and nightside flows dominating during the expansion phase (the flows driven by the release of the stored tail energy and which are therefore associated with the polar cap contraction) (Ref. 39). The question is how large are these oscillations about the mean? In figure 3(a) and 3(b) we show the extreme cases of wholly unbalanced reconnection (on the dayside and nightside, respectively). Such oscillations in the convection pattern are the largest possible, yet we note that the flow pattern when averaged over the whole cycle is very similar in form to a steady-state pattern (figure 3c). Hence we must question the extent to which convection is simply the averaged signature of the substorm cycle.

To investigate this question, figure 9 re-plots the data of Hairston and Heelis (Ref. 6). These authors presented the transpolar voltage, ϕ_{pc} , as a function of the polar cap radius for satellite passes close to the dawn-dusk meridian. In figure 9, this voltage has been replotted as a function of the polar cap flux, F , calculated with the assumption of a circular polar cap, as also used in figures 4 and 6. Each data point is obtained from a single satellite pass (lasting roughly 10 min.). The data show that there is a general tendency for ϕ_{pc} and F to increase together. However, there is also considerable and significant scatter. Because these data take no account of the phase of the substorm cycle, or indeed if any substorm was underway or not, these points therefore represent convection data, in an general sense. Note that for any value of ϕ_{pc} , F can have a wide range of values between F_{min} and F_{max} , as shown by the dashed and dot-dash lines respectively. These lines are reproduced exactly in figures 4 and 6. It is noticeable that the convection data show the same behaviour as during the CDAW6 substorms (fig. 6), and as explained by a simple application of the ECPC model (fig. 4). This suggests that the spread in the convection data in figure 9 is due to the variety of substorm cycle phases included in the convection data. From application of the simple cycle predicted by figure 4 to the data given in figure 9, Lockwood (Ref. 44) has been able to make deductions about the behaviour of the nightside reconnection voltage as a function of the open flux, F .

5. CONCLUSIONS

From application of the ECPC model, a number of conclusions can be drawn about convection and its relationship to the substorm cycle.

- From the variability of the polarity of the IMF B_z component (Refs. 30-32) within the time scales with which the tail reconnection rate (and subsequent energy deposition in the ionosphere) can respond to IMF changes, we must conclude that non-steady conditions will normally apply and steady-state will be rare.

- In non-steady conditions, the open/closed field line boundary will generally move, and flow streamlines (but not the flux tubes and plasma) cross that boundary with no reconnection taking place. Such a boundary is said to be "adiarotic".

● If the adiarocic segments of the open/closed boundary move, the so-called "lobe", "merging" and "viscous" flow cells are not distinct. Only in steady-state (with no polar cap boundary motion) are lobe cells confined to the polar cap and viscous cells confined to the closed field line region, with only merging cells giving flow between these two regions.

● Induction effects caused by merging gap motions mean that the flow voltage seen across the merging gap does not generally equal the reconnection voltage along the corresponding X-line.

● Allowance for induction effects in one example of a substorm indicates that the tail reconnection rate may be driven directly by the orientation of the IMF. Recent statistical studies of other substorms by Goertz et al. (Ref. 47) have also indicated that the so-called "storage" system, may in some respects be directly driven. We note that for this substorm, onset was 30 min. before significant open flux was closed.

● What we term "convection" is actually an average circulation, averaged over the substorm cycle. The flows driven in substorms are not additional perturbations to the convection pattern, rather they are an integral, indeed the dominant, part of this circulation.

REFERENCES

1. Heppner, J.P., 1977, Empirical models of high-latitude electric fields, *J. Geophys. Res.*, **82**, 1115.
2. Volland, H., 1978, A model of the magnetospheric electric convection field, *J. Geophys. Res.*, **83**, 2695.
3. Heelis, R.A., J.K. Lowell, & R.W. Spiro, 1982, A model of the high-latitude ionospheric convection pattern, *J. Geophys. Res.*, **87**, 6339.
4. Heppner, J. P. & N. C. Maynard, 1987, Empirical high-latitude electric field models, *J. Geophys. Res.*, **92**, 4467.
5. Lu, G., P.H. Reiff, M.R. Hairston, R.A. Heelis, & J.L. Karty, 1989, Distribution of convection potential around the polar cap boundary as a function of interplanetary magnetic field, *J. Geophys. Res.*, **94**, 13447.
6. Hairston, M.R. & R.A. Heelis, 1990, Model of the high-latitude ionospheric convection pattern during southward Interplanetary Magnetic Field using DE 2 data, *J. Geophys. Res.*, **95**, 2333.
7. Foster, J.C., 1983, An empirical electric field model derived from Chatanika radar data, *J. Geophys. Res.*, **88**, 981.
8. Oliver, W.L., J.M. Holt, R.H. Ward, and J.V. Evans, Millstone Hill incoherent scatter observations of auroral convection over $60^\circ < L < 75^\circ$: 3. Average patterns versus Kp, *J. Geophys. Res.*, **88**, 5505.
9. Holt, J.M., R.H. Ward, J.V. Evans, & W.L. Oliver, 1987, Empirical models for the plasma convection at high latitudes from Millstone Hill observations, *J. Geophys. Res.*, **92**, 203.
10. Etemadi, A., S.W.H. Cowley, M. Lockwood, B.J.I. Bromage, D.M. Willis, and H. Luehr, 1988, The dependence of high-latitude dayside ionospheric flows on the north-south component of the IMF, a high time resolution correlation analysis using EISCAT "POLAR" and AMPTE UKS and IRM data, *Planet. Space Sci.*, **36**, 471.
11. Friis-Christensen, E., Y. Kamide, A.D. Richmond, & S. Matsushita, 1985, Interplanetary magnetic field control of high-latitude electric fields and currents determined from Greenland magnetometer data, *J. Geophys. Res.*, **90**, 1325.
12. Richmond, A.D., et al., 1988, Mapping electrodynamic features of the high-latitude ionosphere from localised observations: combined incoherent-scatter radar and magnetometer measurements from 18-19 January, 1984, *J. Geophys. Res.*, **93**, 5760.
13. Foster, J.C., H.-C. Yeh, J.M. Holt, and D.S. Evans, 1989, Two-dimensional mapping of dayside convection in *Electromagnetic coupling in the polar clefts and caps*, ed P.E. Sandholt and A. Egeland, Kluwar, pp. 115-125.
14. Knipp, D.J., A.D. Richmond, B. Emery, N.U. Crooker, O. de la Beaujardiere, D. Evans and H. Kroehl, 1991, Ionospheric convection response to changing IMF direction, *Geophys. Res. Lett.*, **18**, 721.
15. Marklund, G.T., L.G. Blomberg, J.S. Murphree, R.D. Elphinstone, L.J. Zanetti, R.E. Erlandson, I. Sandahl, O. de la Beaujardiere, H.J. Opgenoorth and J.F. Rich, 1991, On the electrodynamic state of the auroral ionosphere during northward interplanetary magnetic field: a transpolar arc case study, *J. Geophys. Res.*, **96**, 9567.
16. Lockwood, M., 1991, On flow reversal boundaries and cross-cap potential in average models of high latitude convection, *Planet. Space Sci.*, **39**, 397.
17. Arnoldy, R. L., 1971, Signature in the interplanetary medium for substorms, *J. Geophys. Res.*, **76**, 5189.
18. Baker, D. N., R. D. Zwickl, S. J. Bame, E. W. Hones, Jr., B. T. Tsurutani, E. J. Smith, & S.-I. Akasofu, 1983, An ISEE-3 high time resolution study of the interplanetary parameter correlations with magnetospheric activity, *J. Geophys. Res.*, **88**, 6230.
19. Bargatze, L. F., D. N. Baker, R. L. McPherron & E. W. Hones, Jr., 1985, Magnetospheric impulse response for many levels of geomagnetic activity, *J. Geophys. Res.*, **90**, 6387.
20. Holzer, T.E., R.L. McPherron & D.A. Hardy, 1986, A quantitative empirical model of the magnetospheric flux transfer process, *J. Geophys. Res.*, **91**, 3287.
21. McPherron, R.L., 1972, Substorm related changes in the geomagnetic tail: The growth phase, *Planet. Space Sci.*, **20**, 1521.

22. McPherron, R.L., C.T. Russell, & M.A. Aubry, 1973, Satellite studies of magnetospheric substorms on August 15, 1968, 9. Phenomenological model for substorms, *J. Geophys. Res.*, **78**, 3131.
23. Rostoker, G., S.-I. Akasofu, J.C. Foster, R.A. Greenwald, Y. Kamide, K. Kawasaki, A.T.Y. Lui, R.L. McPherron & C.T. Russell, 1980, Magnetospheric substorms - definitions and signatures, *J. Geophys. Res.*, **85**, 1663.
24. Rostoker, G., S.-I. Akasofu, W. Baumjohann, Y. Kamide, & R.L. McPherron, 1987, The roles of direct input of energy from the solar wind and unloading of stored magnetotail energy during magnetospheric substorms. *Space Sci. Rev.*, **46**, 93.
25. Russell, C.T., 1972, The configuration of the magnetosphere, in *Critical Problems of Magnetospheric Physics*, edited by E.R. Dyer, p.1, Nat. Acad. Sciences, Washington.
26. Russell, C.T. & R.L. McPherron, 1973, The magnetotail and substorms, *Space Sci. Rev.*, **15**, 205.
27. Cowley, S.W.H., 1981, Magnetospheric and ionospheric flow and the interplanetary magnetic field, in *Physical basis of the Ionosphere in the Solar-Terrestrial System*, AGARD CP-295, pp. 4/1-4/14.
28. Cowley, S.W.H., 1983, Interpretation of observed relations between solar wind characteristics and effects at ionospheric altitudes, in *High-Latitude Plasma Physics*, ed. B. Hultqvist and T. Hagfors, pp. 225-249, Plenum Press.
29. Crooker, N.U., 1992, Reverse convection, *J. Geophys. Res.*, in press.
30. Rostoker, G., D. Savoie, & T. D. Phan, 1988, Response of magnetosphere-ionosphere current systems to changes in the interplanetary magnetic field, *J. Geophys. Res.*, **93**, 8633.
31. Hapgood, M. A., Y. Tulunay, M. Lockwood, G. Bowe, & D. M. Willis, 1991, Variability of the interplanetary medium at 1 AU over 24 years: 1963-1986, *Planet. Space Sci.*, **39**, 411.
32. Lockwood, M., 1991, Flux Transfer Events at the dayside magnetopause: Transient reconnection or magnetosheath pressure pulses?, *J. Geophys. Res.*, **96**, 5497.
33. Siscoe, G.L. & T.S. Huang, 1985, Polar cap inflation and deflation, *J. Geophys. Res.*, **90**, 543.
34. Reiff, P.H. and J.L. Burch, 1985, B_y -dependent dayside plasma flow and Birkeland currents in the dayside magnetosphere: 2. A global model for northward and southward IMF, *J. Geophys. Res.*, **90**, 1595.
35. Gosling, J.T., M.F. Thomsen, S.J. Bame, R.C. Elphic & C.T. Russell, 1990, Plasma flow reversals at the dayside magnetopause and the origin of asymmetric polar cap convection, *J. Geophys. Res.*, **95**, 8073.
36. Burch, J.L. 1973, Rate of erosion of dayside magnetic flux based on a quantitative study of polar cusp latitude on the interplanetary magnetic field, *Radio Sci.*, **8**, 955.
37. Moses, J.J., G.L. Siscoe, R.A. Heelis, & J.D. Winningham, 1989, Polar cap deflation during magnetospheric substorms, *J. Geophys. Res.*, **94**, 3785.
38. Lockwood, M. & M.P. Freeman, 1989, Recent ionospheric observations relating to solar-wind-magnetosphere coupling, *Phil. Trans. R. Soc., London, A.*, **328**, 93.
39. Lockwood, M., S.W.H. Cowley, & M.P. Freeman, 1990, The excitation of plasma convection in the high latitude ionosphere, *J. Geophys. Res.*, **95**, 7961.
40. Cowley, S. W. H & M. Lockwood, 1992, Excitation and decay of Solar wind-driven flows in the magnetosphere - ionosphere system, in press, *Annales Geophys.*
41. S.W.H. Cowley, J.P. Morelli, M.P. Freeman, M. Lockwood, & M.F. Smith, 1992, Excitation and decay of flows in the magnetosphere-ionosphere system due to magnetic reconnection at the dayside magnetopause and in the geomagnetic tail, this issue.
42. Lockwood, M. & S.W.H. Cowley, 1991, Comment on "Ionospheric convection response to changing IMF direction" by Knipp et al., *Geophys. Res. Lett.*, **18**, 2173.
43. McPherron, R.L. & R.H. Manka, 1985, Dynamics of the 1054 UT March 2, 1979, substorm event: CDAW 6, *J. Geophys. Res.*, **90**, 1175.
44. Lockwood, M., 1992, Transpolar voltage, convection and the substorm cycle, *J. Geophys. Res.*, to be submitted.
45. Kamide, Y. and W. Baumjohann, 1985, Estimation of the electric fields and currents from International Magnetospheric Study magnetometer data for the CDAW6 intervals: implications for substorm dynamics, *J. Geophys. Res.*, **90**, 1305.
46. Wygant, J. R., R. B. Torbert & F. S. Mozer, 1983, Comparison of S3-2 polar cap potential drops with the interplanetary magnetic field and models of magnetopause reconnection, *J. Geophys. Res.*, **88**, 5727.
47. Goertz, C.K., Lin Hua Shan, and R.A. Smith, 1991, Prediction of geomagnetic activity, University of Iowa report 91-15, submitted to *J. Geophys. Res.*
48. Freeman, M.P. and D.J. Southwood, 1988, The effects of magnetospheric erosion on mid- and high-latitude ionospheric flows, *Planet. Space Sci.*, **36**, 509.